



Electrospun porous materials laden with tea tree oil and zinc nitrate exhibiting tailored physicochemical and *in vitro* apatite formation

Volume 52: 1–17
© The Author(s) 2022
Article reuse guidelines:
sagepub.com/journals-permissions
DOI: 10.1177/15280837221141111
journals.sagepub.com/home/jit


Mohan Prasath Mani¹, Saravana Kumar Jaganathan^{2,3,4} ,
Ahmad Zahran Md Khudzari⁵, Ahmad Fauzi bin Ismail⁶,
Ahmad Athif Mohd Faudzi^{3,4} and Nick Tucker²

Abstract

Scaffold designs must accommodate the complex regeneration processes of damaged bone tissues. We attempt to achieve this goal by developing a composite electrospun scaffold mimicking the structural and functional requirements of extra cellular matrix. This study investigates the use of a novel bone tissue regeneration formulation of tea tree oil (TT) and zinc nitrate Zn_2 incorporated into a polyurethane (PU) nanofibres scaffold fabricated via the well-known electrospinning technique. The diameter of these nanocomposites fibres was smaller (PU/TT-495 \pm 184 nm and PU/TT/(ZnNO₃)₂-409 \pm

¹School of Biomedical Engineering and Health Sciences, Faculty of Engineering, Universiti Teknologi Malaysia, Skudai, Malaysia

²School of Engineering, College of Science, Brayford Pool, Lincoln United Kingdom

³School of Electrical Engineering, Faculty of Engineering, Universiti Teknologi Malaysia, Johor Bahru, Malaysia

⁴Centre for Artificial Intelligence and Robotics, Universiti Teknologi Malaysia, Kuala Lumpur, Malaysia

⁵IJN-UTM Cardiovascular Engineering Center, School of Biomedical Engineering and Health Sciences, Faculty of Engineering, Universiti Teknologi Malaysia, Skudai, Malaysia

⁶Advanced Membrane Technology Research Centre (AMTEC), School of Chemical and Energy Engineering, Universiti Teknologi Malaysia, Skudai, Malaysia

Corresponding author:

Saravana Kumar Jaganathan, School of Engineering, College of Science, Brayford Pool, Lincoln LN6 7TS, United Kingdom.

Email: sjaganathan@lincoln.ac.uk



Creative Commons Non Commercial CC BY-NC: This article is distributed under the terms of the Creative Commons Attribution-NonCommercial 4.0 License (<https://creativecommons.org/licenses/by-nc/4.0/>) which permits non-commercial use, reproduction and distribution of the work without further permission provided the original work is attributed as specified on the SAGE and Open Access pages (<https://us.sagepub.com/en-us/nam/open-access-at-sage>).

155 nm) than polyurethane (1099 ± 118 nm) on its own. Fourier transform infrared spectroscopy analysis revealed that the PU and the additives interact through hydrogen-bond formation. Measuring the wettability of the PU/TT indicated a hydrophobic nature (115 ± 2) which was reversed by the addition of $(\text{ZnNO}_3)_2$ to PU/TT ($69^\circ \pm 2$). TT and the addition of $(\text{ZnNO}_3)_2$ increased the tensile strength. Atomic force microscopy showed that the fibres of PU/TT (633 ± 297 nm) and PU/TT/ $(\text{ZnNO}_3)_2$ (345 ± 147 nm) were smoother than the PU (854 ± 32 nm). The developed nanocomposites showed delayed blood clot activation and reduced toxicity as determined by anticoagulant studies. Further, bone-forming abilities quantified by in vitro calcium deposition studies indicated enhanced calcium deposition (PU/TT-5.6% and PU/TT/ $(\text{ZnNO}_3)_2$ -10.8%) in comparison to PU (2.4%). We have demonstrated that the attributes of these nanocomposites may be successfully exploited for bone reconstruction.

Keywords

polyurethane, $(\text{ZnNO}_3)_2$, tea tree oil, electrospun scaffold, blood compatibility, bone tissue applications

Introduction

Bone replacement is needed to treat bone cysts, tumour ablation, neurosurgical defects and osteolysis.^{1,2} The repairing of damaged bone is challenging and requires multifaceted approaches to achieve successful regeneration. Recently tissue engineered scaffolds have been used to remodel damaged bone tissue aiming to overcome the limitations of conventional strategies such as auto and allografts. These limitations include donor scarcity, immune rejection and infection in the transplanted tissues.^{1,3} Although some setbacks of conventional methods can be overcome, more appropriate scaffolds designs are vital for improved cell adhesion and proliferation. The ideal bone scaffold should possess properties such as biocompatibility, biodegradability, be non-toxic, and exhibit good mechanical strength.^{1,4,5} Although several materials options are available for bone scaffolds, polymer-matrix composites are the most popular for tissue engineering applications due to their versatility and tailor-made properties.^{1,5-7} Further, the developed scaffold should have the potential to mimic^{1,8,9} the three-dimensional ECM structure containing as it does, nano-scale fibrous proteins and proteoglycans.^{1,10}

In designing a scaffold with nano-scale matrices, various fabrication techniques have been employed such as particle leaching, electrospinning, freeze-drying, and gas foaming.⁸ The scaffolds produced by electrospinning are the most common choice for tissue engineering. These electrospun scaffolds produce fibres with a structure closely resembling the structure of native human ECM.⁹ Electrospinning is a cost-effective, versatile and conceptually simple way of fabricating nanofibres using high voltage low current electricity to draw out the fibres.¹¹ The syringe pump loads a blunt hypodermic needle with a solution that is drawn into a fibres by an electrostatic field which may be collected on a grounded target.^{12,13} The fabricated fibre possesses a high surface to

volume ratio and porosity.^{14,15} In this work, the bone scaffold was developed based on synthetic polyurethane polymer as a matrix. Tecoflex EG-80 A has two segments namely methylene bis(cyclohexyl) diisocyanate (hydrogenated MDI, H12MDI) which acts as a hard segment and soft segment as polytetramethylene oxide with a molecular weight of 1000 g/mol. It also contains 1,4 butane diols as a chain extender. Polyurethane scaffolds are widely used in tissue construction because of ease of processing, flexibility, biocompatibility, biodegradable, haemocompatibility, and tailorable chemical and physical forms.¹⁶

A combination of essential oil and metallic particles was added to PU to improve its biological properties. Essential oils (EOs) are extracted through hydro-distillation or steam distillation from various parts of the medicinal plants such as flowers, leaves, barks, roots, and fruits. EOs are composed of various chemical constituents such as alcohols, polyphenols, terpenoids, carbonyl compounds, and aliphatic compounds. These components have been reported to possess various biological properties useful in different applications in the pharmaceutical, agricultural, sanitary, and food industries.¹⁷ Metal ions are known to perform key roles in many critical human bodily functions. It has been reported that a scarcity of certain metal ions leads to illness.¹⁸ Metal ions are reported to possess various biological properties which find application in diagnostics, therapy, anticancer drugs, catalysis, material synthesis and photochemistry.¹⁹

Test polyurethane matrix composites were manufactured with the aim of improving bone-forming abilities by adding TT and zinc nitrate. Tea tree oil-commonly called melaleuca oil is obtained from the *Melaleuca alternifolia* leaves, a native Australian plant.²⁰ TT contains terpene hydrocarbons, sesquiterpenes, and related alcohols.²¹ TT oil possesses therapeutic anti-inflammatory and antimicrobial attributes.²⁰ Some studies report the fabrication of the fibrous scaffolds containing tea tree oil: the composite scaffolds displayed improved tensile strength and long-term antimicrobial effects.^{22,23} Scaffolds incorporating metallic particles are reported to have significantly enhanced tensile strength promoting properties.^{24,25} Zinc (Zn) is a widely used metallic and inorganic material which is reported to have significant antibacterial activity -this property is widely exploited in toothpaste, sunscreens, and textiles.^{26,27} Studies have demonstrated that a fibrous scaffold containing zinc particles will show enhanced blood compatibility, improved cell proliferation, and angiogenesis.^{25,28} Hence, in this study zinc nitrate was chosen to incorporate them into polyurethane matrix.

Scaffolds containing metallic particles are gaining currency,^{25,29,30} the concomitant addition of essential oils is a relatively new concept and may render significantly beneficial properties to the scaffold. We demonstrate the novelty of directly incorporating TT into a PU/(ZnNO₃)₂ scaffold in a simple single step process. The developed scaffold displays remarkable physicochemical properties and bone-forming abilities in vitro which maybe successfully exploited for bone tissue engineering applications.

Experimental procedure

Materials

Tecoflex EG-80 A (molecular weight = 1000 g/mol), a medical-grade thermoplastic PU polymer was supplied from Lubrizol, USA. *N, N*-Dimethylformamide (DMF) was obtained from Merck, Germany. TT was purchased from a local vendor situated at Paradigm Mall, Malaysia and $(\text{ZnNO}_3)_2$ from Sigma Aldrich, Gillingham, UK.

Preparation of PU and composite scaffold

A homogeneous solution of PU was made at 9 wt%, by dissolving 0.450 g of PU in 5 mL of DMF and stirring continuously for 12 h with a magnetic stirrer. Similarly, a homogeneous 4 v/v% solution of tea tree oil was made by dissolving 120 μL in 3 mL of DMF and stirring it for 1 h. A 4 wt% homogeneous solution of zinc nitrate was prepared by adding 0.120 g to 3 mL of DMF and stirring for 1 h. The TT solution was mixed with pure PU solution in the ratio of 1:8 v/v% to fabricate PU/TT spinning dope. Additionally, another composite was fabricated by mixing TT and $(\text{ZnNO}_3)_2$ solution into pure PU solution in the ratio of 0.5:0.5:8 v/v% to fabricate PU/TT/ $(\text{ZnNO}_3)_2$. Pure PU nanofibres, PU/TT, and PU/TT/ $(\text{ZnNO}_3)_2$ scaffold were electrospun using equipment supplied by Progene Link Sdn Bhd, Selangor, Malaysia. All nanofibres were spun at a flow rate of 0.2 mL/h with an applied voltage of 10.5 kV, relative humidity of 55%, and the distance between needle and collector drum was set at 20 cm.

Characterizations

Field emission scanning electron microscope (FESEM). For FESEM analysis (Hitachi SU8020, Tokyo, Japan), small pieces of cut samples (1 cm \times 1 cm) were gold sputtered before imaging. The diameter was estimated by picking 30 individual locations randomly from the image (Image J software).

Fourier transform infrared (FTIR) testing. The functional groups of PU and composite scaffolds were observed using the Nicolet iS 5, Thermo Fischer Scientific, Waltham, MA, USA. A small cut sample (1 cm \times 1 cm) was scanned in the frequency range of 600–4000 cm^{-1} at a resolution of 4 cm^{-1} .

Contact angle measurement

Optima contact angle unit (AST products, Inc., Billerica, MA, USA) was used to investigate the contact angle. A water droplet was placed on the testing membrane (1 cm \times 1 cm) and the liquid drop was viewed through high-resolution video camera. Within a few seconds, an image of the droplet was captured and the angle was computed manually from the software provided with the unit.

Thermogravimetric analysis (TGA). TGA analysis of samples was done by using PerkinElmer TGA 4000 unit (Waltham, MA, USA). Samples weighing 3 mg were heated in a nitrogen atmosphere with a temperature range between 30–900°C at a rate of 10°C/minute.

Atomic force microscopy (AFM). Surface analysis of PU and composite scaffolds was done in AFM unit (Nano Wizard[®], JPK Instruments, Berlin, Germany). A small sample (1 cm × 1 cm) was scanned in tapping mode in a normal ambient atmosphere. The images were scanned in size of 20 μm × 20 μm with a 256-sample resolution.

Tensile testing machine. A Gotech Testing Machines, AI-3000, Taichung City, Taiwan tensile tester was used to investigate the mechanical properties. To begin the test, 4 cm × 1.5 cm samples were pulled at a rate of 10 mm/min with a load of 500 N until failure occurred. The results were plotted as a stress-strain curve and the values of tensile strength were recorded.

Blood compatibility measurements

Blood testing kits were procured from Thermo Fisher Scientific, Selangor, Malaysia, and used as received.

Activated Partial Thromboplastin Time (APTT) Assay. For the APTT assay, a small sample was added with 50 μL of platelet-poor plasma at 37°C for 1 min and then 50 μL of rabbit brain cephaloplastin reagent was added for 3 min at 37°C. After this the mixture was added to 50 μL of calcium chloride (CaCl₂) and the formation time of blood clots was measured using a chronometer.

Prothrombin Time (PT) Assay. For the PT assay, a small piece of the cut sample was added with 50 μL of platelet-poor plasma at 37°C for 1 min and then added with 50 μL of sodium chloride (NaCl)–thromboplastin reagent (Factor III). The activation of the blood clot was done by using the sterile needle and the time taken for blood clot formation was measured using a chronometer.

Haemolysis Assay. Fibre membrane samples were soaked in physiological saline (0.9%w/v) at 37°C for 30 min. For positive control, a complete haemolysis of the whole blood was performed by diluting with distilled water (4:5). Later, the mixture was taken out and centrifuged at 3000 r/min for 15 min. Then, the absorbance of the pipetted clear supernatant was recorded at 541 nm by UV-vis spectroscopy. The haemolysis rate was calculated as reported earlier.^{28,31}

Bioactivity test

Bone forming ability was tested through in vitro apatite formation testing by submerging in simulated body fluid (SBF). The PU, PU/TT, and PU/TT/(ZnNO₃)₂scaffolds were cut

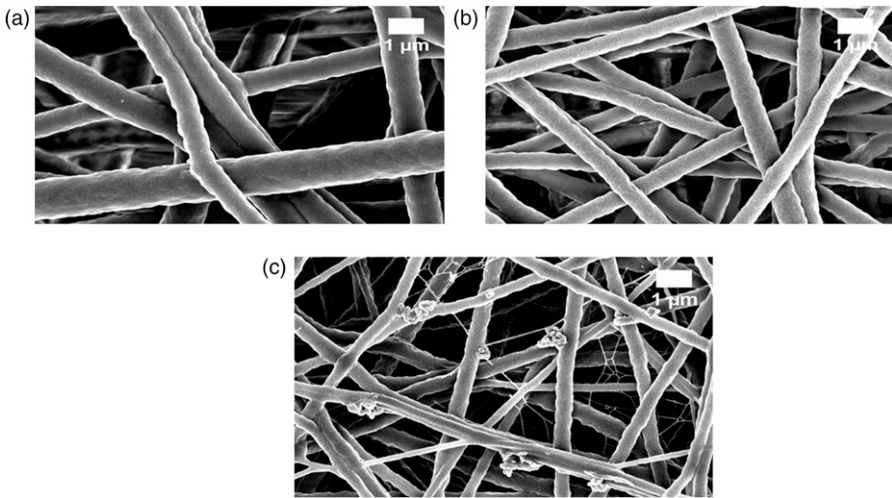


Figure 1. FESEM images of a) PU, b) PU/TT and c) PU/TT/(ZnNO₃)₂.

and left in $1.5 \times$ SBF for 14 days. After 14 days' incubation, the samples were taken and dried. FESEM and Energy Dispersive X-Ray (EDX) analysis was used to calculate the calcium deposited on samples.

Statistical analysis

The experiments were performed three times, a one-way analysis of variance (ANOVA) was executed and results were reported as mean \pm standard deviation. A representative of three independent images is provided by way of quantitative analysis.

Result and Discussion

Field Effect Scanning Electron Microscopy (FESEM) results

FESEM shows the fibrous nature of PU and composite scaffolds as shown in [Figure 1](#).

The scaffolds showed smooth and randomly oriented fibres without bead formation. The nanocomposite scaffolds are smaller in diameter than the PU scaffolds. The mean diameter of the PU fibres were 1099 ± 118 nm whereas PU/TT and PU/TT/(ZnNO₃)₂ were observed to be 495 ± 184 nm and 409 ± 155 nm in diameter. The corresponding fibre diameter distribution curves ($p < 0.05$) are shown in [Figure 2](#). The reduced diameter of the composites is attributed to the presence of TT and (ZnNO₃)₂ in the PU matrix. In a recent study, Mani et al. fabricated a scaffold based on ylang-ylang (*Cananga odorata*) (hereafter YY) oil and zinc nitrate (ZnNO₃)₂ and also observed a fall in diameter of their polyurethane fibres when ZnNO₃ was added. They ascribed the diameter reduction to a change in viscosity of the polymeric composite solution. Further, they concluded that the

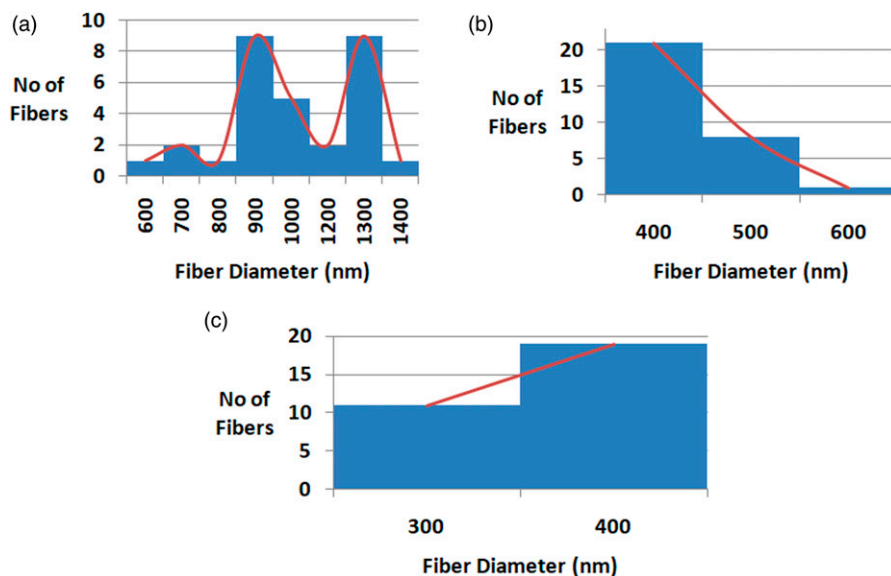


Figure 2. Fibre distribution curve of a) PU, b) PU/TT and c) PU/TT/(ZnNO₃)₂.

fabricated composites were conducive for bone tissue engineering.³¹ Hence, we have some evidence that our PU/TT and PU/TT/(ZnNO₃)₂ exhibiting smaller diameter will be favourable for new bone tissue growth. EDX analysis of the PU and PU/TT scaffolds showed only carbon and oxygen content with no trace of zinc whereas the PU/TT/(ZnNO₃)₂ scaffold showed zinc (1.9%) in addition to the expected oxygen and carbon content.

FTIR analysis

Fourier transform infrared spectroscopy (FTIR) is a universal analytical tool used to identify and characterize the presence of functional groups. FTIR is widely used to classify pure substances, impurities, mixtures, and compositions of various materials.³² Figure 3 shows the results of FTIR analysis of the PU, PU/TT, and PU/TT/(ZnNO₃)₂ scaffolds.

The spectrum of PU sample exhibits main characteristic peaks of NH stretch at 3318 cm⁻¹, CH stretch at 2920 cm⁻¹ and 2852 cm⁻¹ and C = O stretch at 1730 cm⁻¹ and 1701 cm⁻¹. The peak at 1597 cm⁻¹ and 1531 cm⁻¹ are ascribed to NH vibrations, whereas the presence of a peak at 1414 cm⁻¹ denotes CH vibrations. C-O stretch was seen at 1221 cm⁻¹, 1105 cm⁻¹, and 770 cm⁻¹ respectively.^{28,31} The spectra of PU/TT and PU/TT/(ZnNO₃)₂ scaffolds were similar to that of the PU. However, the peak intensity of the composite was increased due to the formation of hydrogen-bonds. This formation of stronger hydrogen bonding was because of the interaction of certain molecules (NH, CH and CO functional groups) present in PU, TT and (ZnNO₃)₂ respectively.³³ Further, the

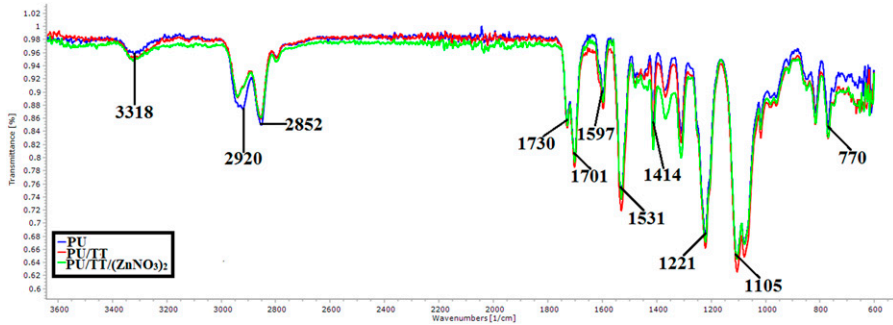


Figure 3. FTIR images of PU, PU/TT and PU/TT/(ZnNO₃)₂.

CH peak shift was also observed when TT and (ZnNO₃)₂ was added to the pristine PU. The CH peak at 2920 cm⁻¹ in PU was shifted to 2939 cm⁻¹ in PU/TT and 2941 cm⁻¹ in PU/TT/(ZnNO₃)₂ respectively.³⁴ The hydrogen bond formation and change in peak positions substantiated the integration of TT and (ZnNO₃)₂.

Contact angle results

Pristine PU scaffold has a contact angle of 105° ± 3, in comparison to PU/TT and PU/TT/(ZnNO₃)₂ which have angles of 115° ± 2 and 69° ± 2 see Figure 4 (*p* < 0.05).

The wettability of the fabricated scaffold could be tailored by the addition of the selected constituents. The addition of TT resulted in the increasing hydrophobic nature of the scaffold, whereas the addition of (ZnNO₃)₂ shifted the scaffolds towards a hydrophilic nature signifying flexibility in tailoring the wettability of the scaffolds. Cui et al. investigated the surface wettability of the poly (D,L-lactide) (PDLA) and poly (D,L-lactide)-poly(ethylene glycol) (PDLA-PEG) electrospun fibres. It has been found that the fibre contact angle is inversely proportional to fibre diameter.³⁵ Further, Ceylan et al. fabricated scaffold using polystyrene and polyvinyl chloride fibres; the water contact angles of the smaller fibre diameter were found to be higher.³⁶ In our nanocomposite PU/TT membrane, the fibre diameter was smaller compared to the pristine PU which should indicate an increase in the

Contact angle. However, the composition of zinc nitrate contains water molecules which might reverse the contact angle favoring hydrophilic behaviour. Finally, it would be interesting to examine the contact angle changes with respect to varying essential oil content. The optimal wettability is needed for the scaffolds in bone tissue formation to enhance osteoblast cell adhesion. Contact angles exceeding 106° would not be conducive for osteoblast growth.³⁷ Though the angle of PU/TT exceeds the optimal wettability, the addition of (ZnNO₃)₂ to the PU/TT scaffold reverted to its optimal value. Hence, the tailor-made wettability of PU/TT/(ZnNO₃)₂ holds potential in favouring the proliferation of osteoblast cells.

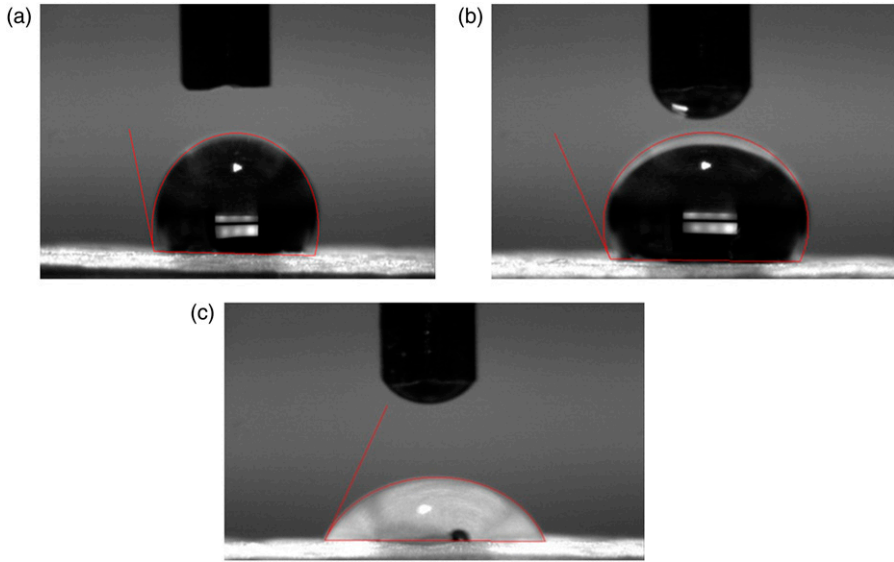


Figure 4. Contact angle images of (a) PU, (b) PU/TT and (c) PU/TT/(ZnNO₃)₂.

Thermo-gravimetric analysis (TGA) results

Thermal analysis of materials fabricated for tissue engineering applications has been used to analyze degradation behavior.^{38,39} A thermal analysis study was used to determine thermal stability, the interaction of added additives, and general integrity.⁴⁰ Figures 5 and 6 show the thermal curve of our PU and its composites. The initial onset of degradation was higher for PU (284°C) compared to PU/TT (295°C) ($p < 0.05$). PU/TT/(ZnNO₃)₂ displayed slightly lower (260°C) than both ($p < 0.05$).

TT enhanced the thermal stability of the PU whilst adding (ZnNO₃)₂, decreased stability because of the evaporation of water of hydration from the zinc nitrate. The Derivative Thermogravimetric (DTG) curve depicts weight loss curves in which PU scaffold exhibited three weight loss peaks similar to PU/TT and PU/TT/(ZnNO₃)₂. The intensity of weight loss was reduced in PU/TT and PU/TT/(ZnNO₃)₂ than PU indicating their improved thermal stability. These observations further corroborated the presence of TT and (ZnNO₃)₂ in the polyurethane.

Surface roughness results

Figure 7 shows 3D images of PU, PU/TT and PU/TT/(ZnNO₃)₂ scaffold surfaces. The pristine PU showed an average roughness of 854 ± 32 nm. PU/TT and PU/TT/(ZnNO₃)₂ nanocomposites exhibited an average roughness of 633 ± 297 nm and 345 ± 147 nm respectively ($p < 0.05$). Both composites had low roughness due to the constituents of TT and (ZnNO₃)₂ integrating with the PU. Kim et al. fabricated electrospun scaffolds from

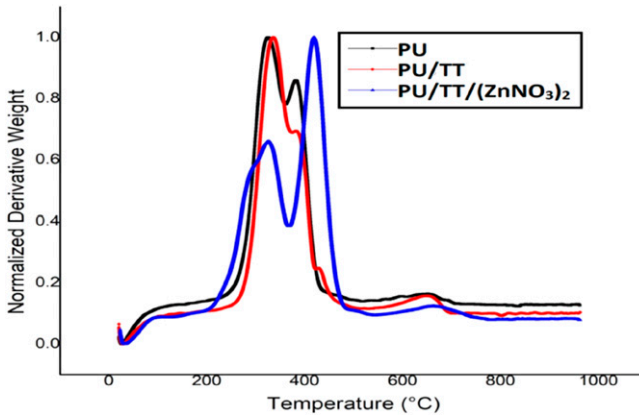


Figure 5. TGA curve of (a) PU, PU/TT and PU/TT/(ZnNO₃)₂.

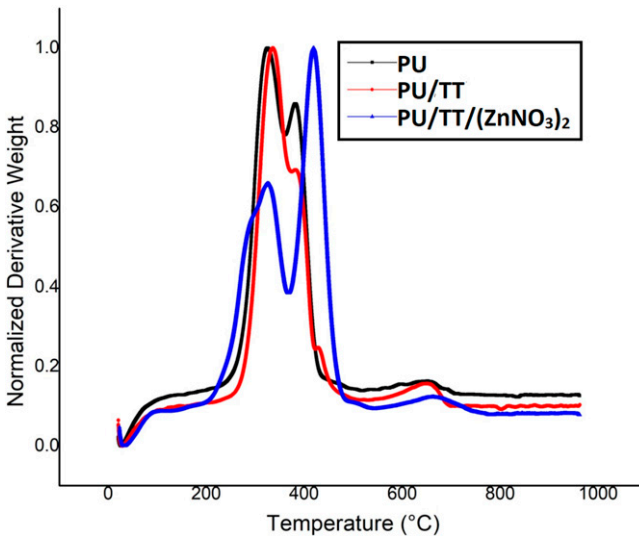


Figure 6. DTG curve of PU, PU/TT and PU/TT/(ZnNO₃)₂.

poly (ϵ -caprolactone) (PCL) and reported that their fabricated scaffolds with smaller diameter

showed smoother surfaces compared to the larger diameter ones. Our observations were similar to those findings and the added constituents might reasonably affect the fibre diameter.⁴¹ Hence, the fabricated composites consist of smaller diameter fibres which maybe the reason for smoother surfaces. Ribeiro et al. reported that the poly (l-lactide) (PLA) scaffolds enhanced osteoblast cell proliferation by providing smoother surfaces.⁴²

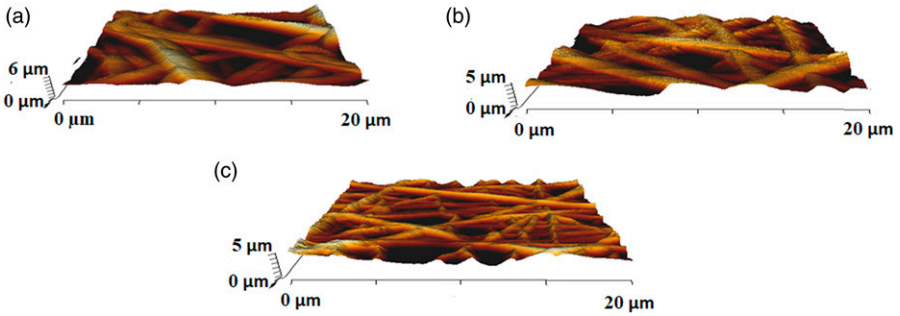


Figure 7. Surface roughness of (a) PU, (b) PU/TT and (c) PU/TT/(ZnNO₃)₂.

Hence, smooth surfaces of PU/TT and PU/TT/(ZnNO₃)₂ may reasonably be assumed to be beneficial for bone growth.

Tensile testing

Figure 8 shows the tensile test results for PU, PU/TT, and PU/TT/(ZnNO₃)₂ scaffolds. The tests show an increase in the tensile strength of pristine PU with the addition of TT and (ZnNO₃)₂. PU alone showed a tensile strength of about 6.16 MPa, while the PU/TT and PU/TT/(ZnNO₃)₂ nanocomposites are stronger at 9.81 MPa and 13.03 MPa respectively ($p < 0.05$). The mean and standard deviations for the tensile strength of the electrospun membranes are shown in Table 1.

Unnithan et al. developed a skin scaffold based on polyurethane added with emu oil (rendered fat from *Dromaius novaehollandiae*). The addition of emu oil resulted in an increase in tensile strength of the pure PU which correlates with our findings. They linked this behavior to the cohesive properties of emu oil augmenting the tensile strength. Further, they also concluded that the fibre attachment was due to the formation of hydrogen bonding between PU and emu oil molecules. In our study, TT might have possessed a similar cohesive property which would augment fibre attachment owing to the hydrogen bonding between TT and PU and thus increasing tensile strength. Jeon et al. developed a nano-fibrous scaffold based on PU/PCL incorporated with silver nanoparticles. It was observed that the tensile strength of the nano-fibrous PU/PCL scaffold was increased by the addition of the silver nanoparticles. They attributed to the increase in tensile strength to a decrease in fibre diameter. In our study, the electrospun nanocomposites were smaller in fibre diameter than the pristine PU, resulting in a likely increase in tensile strength. Commercially available bone substitutes are autograft tissue from the patient, allograft tissue from a human donor, or xenograft tissue from an animal. Being derived from mammalian bone, their main composition is hydroxyapatite (HA). The reported tensile strength of nano HA scaffold was in the range of 3–10 MPa.^{43,44} Further, tensile strengths of electrospun membranes for bone scaffolds have been reported in the range of 4 MPa.^{45,46} The observed strength of our PU/TT and PU/TT/(ZnNO₃)₂ scaffolds matched the values increasingly required for bone reconstruction.

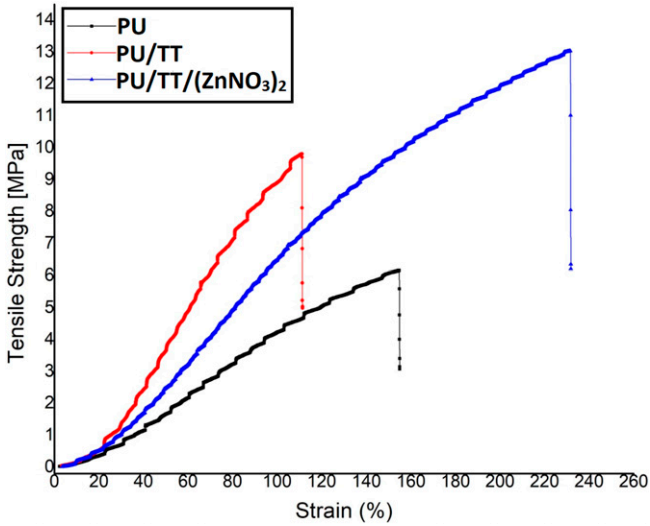


Figure 8. Tensile curves of PU, PU/TT and PU/TT/(ZnNO₃)₂.

Table I. Mean and standard deviation of tensile strength for the electrospun membranes.

Sample	Tensile strength (MPa)
PU	5.89 ± 0.28
PU/TT	8.77 ± 0.734
PU/TT/(ZnNO ₃) ₂	12.68 ± 0.907

Blood compatibility measurements

In clinical applications, blood compatibility assessment determines the expected failure level of fabricated membranes. When the test material contacts blood, platelet surface interaction will take place as a result of the rapid absorption of plasma proteins. This platelet surface interaction might lead to thrombus formation and the consequent failure of the test material.⁴⁷ Blood clotting times of the PU and composite scaffolds were quantified by APTT and PT assay and their results are shown in Figures 9(a) and (b). The observed APTT time for PU was 176 ± 2 s and PU/TT and PU/TT/(ZnNO₃)₂ showed 205 ± 3 s and 200 ± 1 s respectively ($p < 0.05$). Similarly, PT time for the pristine PU was observed at 94 ± 2 s and for the PU/TT and PU/TT/(ZnNO₃)₂ was estimated to be 109 ± 1 s and 106 ± 1 s ($p < 0.05$). The alteration in the clotting times is because of TT and (ZnNO₃)₂ added in the PU.

The hydrophobic PU/TT showed a higher clotting time. In hydrophobic surfaces, permanent adhesion of plasma proteins forms a surface layer that prevents further cell adhesion, and delays clotting time. The decrease in clotting time of PU/TT/(ZnNO₃)₂ is attributed to changes in polar and apolar regions.⁴⁸ PU/TT and PU/TT/(ZnNO₃)₂ scaffolds

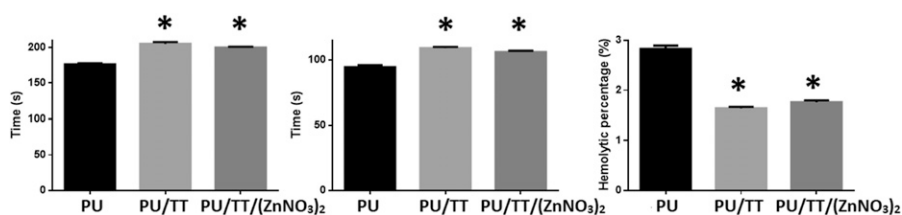


Figure 9. (a) APTT, (b) PT and (c) Haemolytic index of PU, PU/TT and PU/TT/(ZnNO₃)₂.

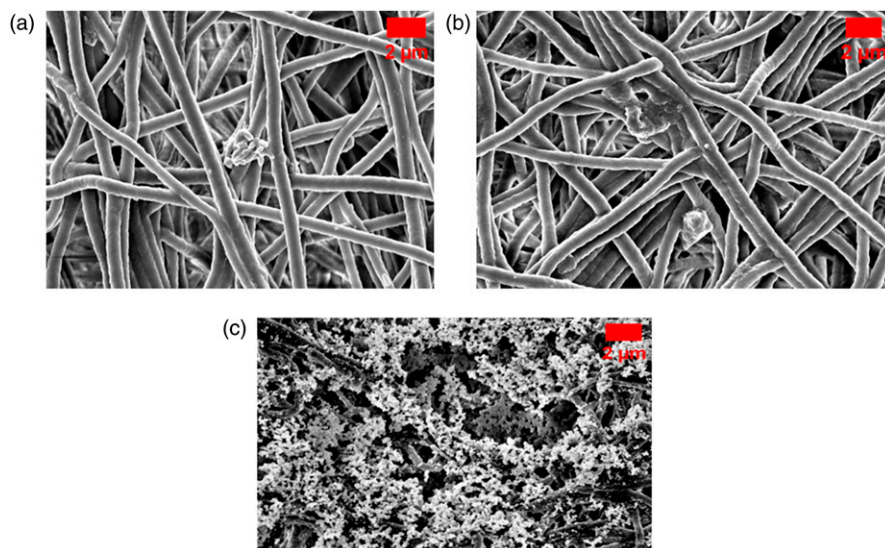


Figure 10. FESEM images of bone mineralisation in the electrospun membranes (a) PU, (b) PU/TT and (c) PU/TT/(ZnNO₃)₂.

Table 2. EDX table of bone mineralisation in the electrospun membranes (a) PU, (b) PU/TT and (c) PU/TT/(ZnNO₃)₂.

Element	PU		PU/TT		PU/TT/(ZnNO ₃) ₂	
	Wt%	Σ	Wt%	Σ	Wt%	σ
C	74.4	0.6	65.3	1	44.5	1
O	22.1	0.5	26	0.8	35.9	0.9
Ca	2.4	0.3	7.5	0.7	12.9	0.9
P	1	0.3	1.2	0.4	6.7	0.6

displayed haemolytic percentages of 1.64% and 1.76%. PU showed a higher index value of 2.83% - see Figure 9(c) ($p < 0.05$). The newly formed materials behave as a non-haemolytic material according to ASTM F756-00 (2000).^{28,31} Haemocompatibility is a multifaceted phenomenon and is found to be influenced by physical, chemical, and surface properties. It has been reported that scaffold properties such as fibre diameter, surface roughness, and wettability behaviour all influence blood compatibility.⁴⁹ In our study, the reduced diameter (both composites) and hydrophobic nature (PU/TT)⁵⁰ of the developed nanocomposite resulted in anticoagulant properties.

Bone mineralization testing

The amount of calcium deposited on the PU, PU/TT, and PU/TT/(ZnNO₃)₂ was determined using bone mineralization testing. Figure 10 and Table 2 show the corresponding FESEM image and EDX table of the fabricated scaffolds after 14 days in Simulated Body Fluid (SBF). The amount of calcium deposited on the PU was 2.4% and for electrospun PU/TT and PU/TT/(ZnNO₃)₂ 7.5% and 12.9% respectively ($p < 0.05$). Andric *et al.* developed electrospun poly (L-lactide) (PLLA) scaffolds and also investigated bone mineralization. Membranes of gelatin incorporated PLLA showed a higher degree of calcium phosphate mineral precipitation—a condition favourable for bone tissue engineering.⁵¹ Hence, the acceleration of calcium deposition caused by the addition of TT and (ZnNO₃)₂ to the PU indicating great promise for bone reconstruction.

Conclusion

This study presents the fabrication and characterization of new composite based on polyurethane with active ingredients of tea tree (*Melaleuca alternifolia*) oil and zinc nitrate. The additive modified polyurethane displayed a significant change in physico-chemical properties and beneficial alteration of mechanical properties, namely an incremental percentage of 59.25% for PU/TT and 111.53% for PU/TT/(ZnNO₃)₂, coupled with a decrease in toxicity of 42.05% for PU/TT and 37.81% for PU/TT/(ZnNO₃)₂, and an increase in bone-forming abilities of 212.5% for PU/TT and 437.5% for PU/TT/(ZnNO₃)₂. This demonstrates a high degree of potential suitability of PU/TT and PU/TT/(ZnNO₃)₂ scaffolds for bone tissue engineering. However, further evaluation of potential using osteoblast cells and in vivo animal testing is required to confirm these materials as suitable candidates for bone tissue engineering.

Conflict of interest

The author(s) declared no potential conflicts of interest with respect to the research, authorship, and/or publication of this article.

Funding

The author(s) received no financial support for the research, authorship, and/or publication of this article.

ORCID iD

Saravana Kumar Jaganathan  <https://orcid.org/0000-0002-2785-137X>

References

1. Qi J, Zhang H, Wang Y, et al. Development and blood compatibility assessment of electrospun polyvinyl alcohol blended with metallocene polyethylene and *Plectranthusamboinicus* (PVa/mPe/Pa) for bone tissue engineering. *Int J Nanomed* 2018; 13: 2777.
2. Ong KL. New biomaterials for orthopedic implants. *Int J Nanomed* 2015; 7: 107–130.
3. Zhao L, Zhao J-L, Wan L, et al. The study of the feasibility of segmental bone defect repair with tissue-engineered bone membrane: a qualitative observation. *Strat Trauma Limb Reconstr* 2008; 3(2): 57–64.
4. O'Brien FJ. Biomaterials & scaffolds for tissue engineering. *Mater Today* 2011; 14(3): 88–95.
5. Dhandayuthapani B, Yoshida Y, Maekawa T, et al. Polymeric scaffolds in tissue engineering application: a review. *Int J Polym Sci* 2011; 2011: 1–19.
6. Sheikh Z, Najeeb S, Khurshid Z, et al. Biodegradable materials for bone repair and tissue engineering applications. *Mater* 2015; 8(9): 5744–5794.
7. Kar KK, Rana S and Pandey J. *Handbook of Polymer Nanocomposites Processing; Performance and Application*. Berlin, Heidelberg: Springer-Verlag, 2015, pp. 1–601.
8. Eltom A, Zhong G and Muhammad A. Scaffold techniques and designs in tissue engineering functions and purposes: a review. *Adv Mater Sci Eng* 2019; 2019. [10.1155/2019/3429527](https://doi.org/10.1155/2019/3429527): 13.
9. Wang X, Ding B and Li B. Biomimetic electrospun nanofibrous structures for tissue engineering. *Mater Today* 2013; 16(6): 229–241.
10. Heydarkhan-Hagvall S, Schenke-Layland K, Dhanasopon AP, et al. Three-dimensional electrospun ECM-based hybrid scaffolds for cardiovascular tissue engineering. *Biomater* 2008; 29(19): 2907–2914.
11. Rogina A. Electrospinning process: versatile preparation method for biodegradable and natural polymers and biocomposite systems applied in tissue engineering and drug delivery. *Appl Surf Sci* 2014; 296: 221–230.
12. Alghoraibi I and Alomari S. Different methods for nanofibre design and fabrication. In: *Handbook of Nanofibres*: Springer, Cham, 2018: 1–46.
13. Mirek A, Korycka P, Grzeczkwicz M, et al. Polymer fibres electrospun using pulsed voltage. *Mater Des* 2019; 183: 108106.
14. Vasita R and Katti DS. Nanofibres and their applications in tissue engineering. *Int J Nanomed* 2006; 1(1): 15.
15. Liu C, Wong HM, Yeung KW, et al. Novel electrospun polylactic acid nanocomposite fibre mats with hybrid graphene oxide and nanohydroxyapatite reinforcements having enhanced biocompatibility. *Polym* 2016; 8(8): 287.
16. Joseph J, Patel RM, Wenham A, et al. Biomedical applications of polyurethane materials and coatings. *Trans IMF* 2018; 96(3): 121–129.
17. Reddy DN. *Essential oils extracted from medicinal plants and their applications*. Innat Bioactive Compounds 2019: 237–283. Chapter 9.
18. Gupta SP. Roles of metals in human health. *MOJ Bioorg Org Chem* 2018; 2(5): 221–224.

19. Jurca T, Marian E, Vicaş LG, et al. Metal complexes of pharmaceutical substances. In: *Spectroscopic Analyses - Developments and Applications* 2017: 123–142. Chapter 7.
20. Available at: <https://www.medicalnewstoday.com/articles/262944.php>
21. Carson CF, Hammer KA and Riley TV. Melaleuca alternifolia (tea tree) oil: a review of antimicrobial and other medicinal properties. *Clin Microbiol Rev* 2006; 19(1): 50–62.
22. Ge Y, Tang J, Fu H, et al. Characteristics, controlled-release and antimicrobial properties of tea tree oil liposomes-incorporated chitosan-based electrospun nanofibre mats. *Fibres Polym* 2019; 20(4): 698–708.
23. Zhang W, Huang C, Kusmartseva O, et al. Electrospinning of polylactic acid fibres containing tea tree and manuka oil. *React Functpolym* 2017; 117: 106–111.
24. Jaganathan SK and Mani MP. Electrospun polyurethane nanofibrous composite impregnated with metallic copper for wound-healing application. *3 Biotech* 2018; 8(8): 327.
25. Augustine R, Dominic EA, Reju I, et al. Investigation of angiogenesis and its mechanism using zinc oxide nanoparticle-loaded electrospun tissue engineering scaffolds. *RSC Adv* 2014; 4(93): 51528–51536.
26. Sirelkhatim A, Mahmud S, Seeni A, et al. Review on zinc oxide nanoparticles, antibacterial activity and toxicity mechanism. *Nano-Micro Letters* 2015; 7(3): 219–242.
27. Kent JA. *Handbook of Industrial Chemistry and Biotechnology*. Springer Science & Business Media, Berlin, Germany 2013.
28. Jaganathan SK and Mani MP. Single-stage synthesis of electrospun polyurethane scaffold impregnated with zinc nitrate nanofibres for wound healing applications. *J Applpolym Sci* 2019; 136(3): 46942.
29. Kumari S, Singh BN and Srivastava P. Effect of copper nanoparticles on physico-chemical properties of chitosan and gelatin-based scaffold developed for skin tissue engineering application. *3 Biotech* 2019; 9(3): 1–4.
30. de Laia AG, Barrioni BR, Valverde TM, et al. Therapeutic cobalt ion incorporated in poly (vinyl alcohol)/bioactive glass scaffolds for tissue engineering. *J Mater Sci* 2020; 55(20): 8710–8727.
31. Mani MP, Jaganathan SK and Supriyanto E. Enriched Mechanical Strength and Bone Mineralisation of Electrospun Biomimetic Scaffold Laden with Ylang-Ylang Oil and Zinc Nitrate for Bone Tissue Engineering. *Polym* 2019; 11(8): 1323.
32. Kowalczyk D and Pitucha M. Application of FTIR method for the assessment of immobilization of active substances in the matrix of biomedical materials. *Mater* 2019; 12(18): 2972.
33. Unnithan AR, Pichiah PT, Gnanasekaran G, et al. Emu oil-based electrospun nanofibrous scaffolds for wound skin tissue engineering. *Colloids Surf A: Physicochem Eng Asp* 2012; 415: 454–460.
34. Tijing LD, Ruelo MTG, Amarjargal A, et al. Antibacterial and superhydrophilic electrospun polyurethane nanocomposite fibres containing tourmaline nanoparticles. *Chem Eng* 2012; 197: 41–48.
35. Cui W, Li X, Zhou S, et al. Degradation patterns and surface wettability of electrospun fibrous mats. *Polymdegrad Stab* 2008; 93(3): 731–738.
36. Ceylan M. *Superhydrophobic Behavior of Electrospun Nanofibres with Variable Additives*. Doctoral dissertation, Wichita State University, Wichita 2009.

37. Wei J, Igarashi T, Okumori N, et al. Influence of surface wettability on competitive protein adsorption and initial attachment of osteoblasts. *Biomed Mater* 2009; 4(4): 045002.
38. Heydari Z, Mohebbi-Kalhari D and Afarani MS. Engineered electrospun polycaprolactone (PCL)/octacalcium phosphate (OCP) scaffold for bone tissue engineering. *Mater Sci Eng* 2017; 81: 127–132.
39. Chahal S, Hussain FS, Yusoff MM, et al. Nanohydroxyapatite-coated hydroxyethyl cellulose/poly (vinyl) alcohol electrospun scaffolds and their cellular response. *Int J Polym Mater Polymbiomater* 2017; 66(3): 115–122.
40. Mani MP, Jaganathan SK, Khudzari AZ, et al. Development of advanced nanostructured polyurethane composites comprising hybrid fillers with enhanced properties for regenerative medicine. *Polym Test* 2019; 73: 12–20.
41. Kim HH, Kim MJ, Ryu SJ, et al. Effect of fibre diameter on surface morphology, mechanical property, and cell behavior of electrospun poly (ϵ -caprolactone) mat. *Fibres Polym* 2016; 17(7): 1033–1042.
42. Ribeiro C, Sencadas V, Areias AC, et al. Surface roughness dependent osteoblast and fibroblast response on poly (l-lactide) films and electrospun membranes. *J Biomed Mater Res A* 2015; 103(7): 2260–2268.
43. Salifu AA, Lekakou C and Labeed FH. Electrospun oriented gelatin-hydroxyapatite fibre scaffolds for bone tissue engineering. *J Biomed Mater Res Part A* 2017; 105(7): 1911–1926.
44. Kostopoulos V, Kotrotsos A, Fouriki K, et al. Fabrication and Characterization of Poly-etherimide Electrospun Scaffolds Modified with Graphene Nano-Platelets and Hydroxyapatite Nano-Particles. *Int J Mole Sci* 2020; 21(2): 583.
45. Chahal S, Hussain FS, Kumar A, et al. Electrospun hydroxyethyl cellulose nanofibres functionalized with calcium phosphate coating for bone tissue engineering. *RSC* 2015; 5(37): 29497–29504.
46. Shanmugavel S, Reddy VJ, Ramakrishna S, et al. Precipitation of hydroxyapatite on electrospun polycaprolactone/aloe vera/silk fibroin nanofibrous scaffolds for bone tissue engineering. *J Biomaterappl* 2014; 29(1): 46–58.
47. Mao C, Qiu Y, Sang H, et al. Various approaches to modify biomaterial surfaces for improving hemocompatibility. *Adv Colloid Interf Sci* 2004; 110(1–2): 5–17.
48. Szycher M. *High Performance Biomaterials: A Complete Guide to Medical and Pharmaceutical Applications*. Boca Raton: CRC Press, 1991, pp. 1–824.
49. Huang N, Yang P, Leng YX, et al. Hemocompatibility of titanium oxide films. *Biomater* 2003; 24(13): 2177–2187.
50. Li G, Li P, Chen Q, et al. Enhanced mechanical, thermal and biocompatible nature of dual component electrospun nanocomposite for bone tissue engineering. *Peer J* 2019; 7: e6986.
51. Andric T, Wright LD and Freeman JW. Rapid mineralization of electrospun scaffolds for bone tissue engineering. *J Biomater Sci Polym Ed* 2011; 22(11): 1535–1550.